Further investigation of sedimentation velocities of graupel and snow in the WRF Single-Moment 6-Class Microphysics scheme (WSM6)

Kyo-Sun Sunny Lim*, Song-You Hong*, Jimy Dudhia**

*Global Environment Laboratory, Department of Atmospheric Sciences,
Yonsei University, Seoul, Korea

** Mesoscale and Microscale Meteorology Division, National Center for Atmospheric Research,
Boulder, Colorado, USA

1. Introduction

Hong and Lim (2006) developed WRF Single-Moment 6-Class Microphysics scheme (WSM6) having a revised ice process treatment suggested by Hong *et al.* (2004). WSM6 follows the bulk microphysics approach that represents hydrometeor size for the each class with a distribution of function, such as a exponential function or a gamma type resulting in much fewer prognostic variables. Simplified formulas represent all interactions between each of the hydrometeor classes which result from the integration of the hydrometeor spectra. Microphysical processes among the 6 hydrometeors (cloud water, cloud ice, rain, snow, graupel, and snow) in the WSM6 closely follow those of Lin *et al.* (1983) and Rutledge and Hobbs (1984). The microphysical properties of WSM6 scheme are demonstrated in Fig. 1. Each source/sink term in Fig. 1 is described in the paper by Hong and Lim in detail (2006).

The WSM6 scheme has been one of the microphysics options in the WRF model since 2004. The scheme has been widely evaluated at NCAR and showed a good performance against the Purdue-Lin scheme in resolving precipitation convective systems (Klemp 2006, Kuo 2006). But sometimes WSM6 underestimates the snow and overestimates the graupel under the warm temperature-circumstance. Also it is reported that WSM6 has less cloud water over the whole vertical level, compared with observation (Lin *et al.* 2006, Otkin *et al.* 2006).

Barthazy (2004) mentioned the existence of mixed phase of graupel with snow flake in the atmosphere. If we adopt new velocities for the snow and graupel based on the observational evidence, the vertical distribution of hydrometeors affected directly from the bulk microphysics schemes can be changed. The ultimate goal of this research reported in this paper is to improve the weakness of WSM6 mentioned earlier by including the fact, that is co-existence of snow and graupel, into the WSM6.
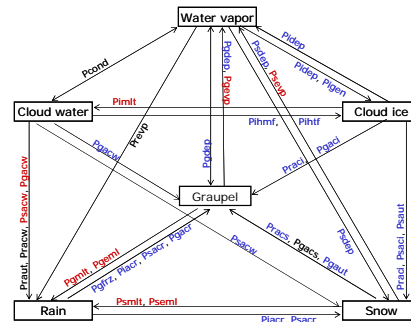

Fig. 1 Flowchart of the microphysics processes in the WSM6 scheme. The terms with red (blue) colors are activated when the temperature is above (below) 0℃, whereas the terms with black color are in the entire regime of temperature.

2. Numerical Experimental Setup

The model used in this study is the Advanced Research WRF (ARW; Skamarock *et al.,* 2005) version 2.1.2, which was released in January 2006. Two sets of experiments were conducted using an idealized 2D thunderstorm case and a 3D real-data simulation of a heavy rainfall event over Korea. And Four experiments are carried out for each case (Table 1), Experiment1 (Exp1) employs the WSM6 microphysics scheme which has changed accretion process for the snow as compared with that of Hong and Lim (2006) (i.e., accretion of cloud water by snow works as a source term for snow, not for graupel). Exp1 experiment results in more cloud water in the middle atmosphere as compared with Hong and Lim (2006), but the effect is not significant. In the experiment2 (Exp2), the velocities of snow and graupel used in calculation of several accretion processes is given by

$$\bar{V}_{gs}[\text{ms}^{-1}] = \frac{q_s\bar{V}_s + q_g\bar{V}_g}{q_s + q_g} \qquad (1)$$

where $\bar{V}_s$ and $\bar{V}_g$ indicate the mass weighted velocities of snow and graupel respectively. Those

are of the form:

$$\overline{V}_s[\text{ms}^{-1}] = \frac{a_s \Gamma(4+b_s)}{6}\left(\frac{\rho_o}{\rho}\right)^{\frac{1}{2}} \frac{1}{\lambda_s^{b_s}}$$

And (2)

$$\overline{V}_g[\text{ms}^{-1}] = \frac{a_g \Gamma(4+b_g)}{6}\left(\frac{\rho_o}{\rho}\right)^{\frac{1}{2}} \frac{1}{\lambda_g^{b_g}}$$ (3)

Where a_s, b_s are the empirical formulas of fall speed for snowflakes having diameter D_s, and a_g, b_g for the graupel. And λ indicates the slope of each hydrometeor size distribution. Formula (1) is based on the observational evidence (ie., there exists mixed phase of graupel with snow flake). Figure 2 shows that the new velocity of snow (graupel) is faster (slower) than the old one irrespective of the amount of mixing ratio of hydrometeor. Experiment 3(Exp3) also adopts new velocities for the snow and graupel, but new ones work only for the sedimentation processes of snow and graupel. And Experiment 4 (Exp4) applies new velocity to the accretion and sedimentation processes of snow and graupel.

Table 1. Summary of sensitivity experiments for the new velocities of snow and graupel.

Code	Description
Exp1	WSM6 microphysics (accretion of cloud water by snow works as a source term for snow, not for graupel, if $T \le T_0$
Exp2	No accretion between the snow and graupel
Exp3	Changed sedimentation term of snow/graupel
Exp4	Exp2+Exp3

a. Idealized thunderstorm experiment

The idealized thunderstorm experiment was designed to systematically distinguish differences between the experiments explained in table 1 by the virtue of fixed initial conditions and the absence of other non-microphysical processes, which in turn would help us to understand the impact of the changes in the velocities of snow and graupel in the 3D framework. A detailed experimental setup follows the Hong and Lim (2006)

b. Heavy rainfall experiment

A significant amount of precipitation was recorded in Korea on July 15, 2001, with a local maximum of approximately 371.5 mm near Seoul (Fig. 3a). Most of the rainfall was observed during the 12-h period from 1200 UTC July 14 to 0000 UTC July 15, 2001, and the maximum rainfall intensity was 99.5 mmh^{-1}. During the heavy precipitation, the high-pressure systems located on the northern side of the peninsula prevented the monsoon front from moving northward, restricting it to Korea.

In association with the significant rainfall over Korea, the upper level large-scale features (not shown) indicated the strengthening of the southerly low-level jet (LLJ) bringing moisture northward to the heavy precipitation region and the intensification of baroclinicity in the mid-troposphere. The heavy precipitation region was located south of the exit of the upper-level jet. A more detailed synoptic overview related to this case is available in the report by Lim and Hong (2005) and Hong and Lim (2006).

In this study, the physics packages include the WSM6 microphysics scheme (Hong and Lim, 2006), the Kain-Fritsch (1993) cumulus parameterization scheme, the Noah land-surface model (Chen and Dudhia, 2001), the Yonsei University planetary boundary layer (PBL) (Hong et al., 2006), a simple cloud-interactive radiation scheme (Dudhia, 1989), and Rapid Radiative Transfer Model (RRTM) longwave radiation (Mlawer et al., 1997) schemes.

The model configuration consisted of a nested domain configuration defined in the Lambert conformal space (Fig. 3b). A 5-km model covering the Korean peninsula (Domain 3, 181 × 181), was surrounded by a 15-km grid model (Domain 2, 100 × 100), which in turn was surrounded by a 45-km grid model (Domain 1, 80 × 80) by a one-way interaction. All grid systems had 23 vertical layers and the model top was located at 50 mb. No cumulus parameterization was used at the 5-km grid model.
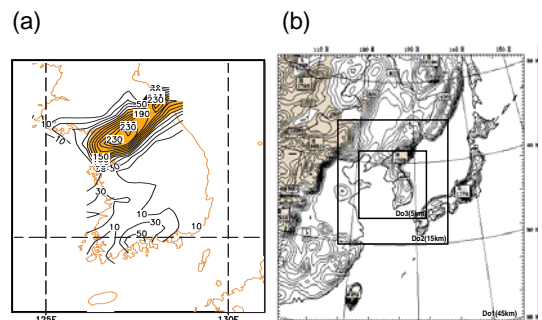
(a) (b)

Fig. 3 (a) Observed 24-h accumulated precipitation (mm) valid at 0000 UTC 15 July 2001, and (b) model terrain contoured every 100m for 45-km (D01). The resolutions of inner domains (D02 and D03) are 15-km and 5-km. Terrain heights greater than 1000 m are shaded.

Initial and boundary conditions are based on the NCEP-NCAR reanalysis (Kalnay et al., 1996).

The simulations were executed from 0000 UTC July 14 to 0000 UTC July 15, 2001, which is forced by the reanalysis data that are available at 6-hour intervals.

3. Results

a. Idealized thunderstorm experiment

Figure 4 compares the condensation fields from the experiments conducted in this study. All experiments simulate the general structure of the thunderstorm, such as the cloud/ice water in the updraft region near the storm center and anvil cloud well. The Exp2 and Exp4 produce more snow field than the Exp1 experiment around freezing level (Figs. 4b and d). This fact is mainly due to the loss of accretion term of snow by graupel (pgacs) among the several changed accretion term. The absence of pgacs term caused by new velocity leads more (less) snow (graupel) to remain at around freezing level of atmosphere. Figure 4c and d show the effect of new velocity for the sedimentation process in the WSM6 microphysics scheme. The less snow mixing ratio at the upper part of atmosphere in the both experiments is due to the faster velocity of snow than the Exp1 experiment.
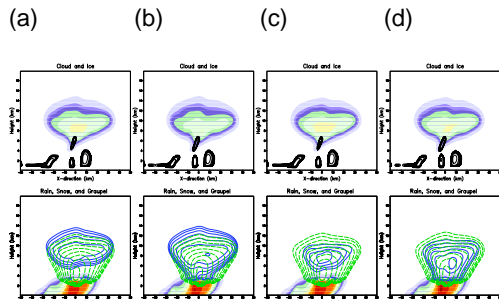
(a)   (b)   (c)   (d)

Fig. 4 Isolines of the condensation fields for cloud particles (first low), cloud ice (shaded), cloud water (solid), and for precipitable particles (second row), rain (shaded), snow (short dashed) and graupel (long dashed), from the (a) Exp1, (b) Exp2, (c) Exp3, and (d) Exp4 experiments. Contour lines are at 0.01, 0.02, 0.04, 0.08, 0.16, 1.28, 2.56, 5.12, and 10.24 gkg^{-1}.

Sensitivity tests of changed velocities of snow and graupel do not change much about the condensation fields of cloud water and cloud ice. But we can found out that there exists more cloud water at around freezing level in the Exp2 and Exp4 experiments (Figs. 4b and d). The amount of cloud water in the middle atmosphere is affected by accretion processes of cloud water by other hydrometeors (especially the accretion of cloud

water by snow (psacw) and the accretion of cloud water by graupel (pgacw)) those are activated when the temperature is below 0 degree. More amount of snow and graupel leads the accretion processes inefficient, because the formula of psacw and pgacw is inverse proportion of the amount of each hydrometeor. New velocities for the snow and graupel cause more snow remained around at 3-5km along the vertical level. Thus more snow results in more cloud water remained around this level in the Exp2 and Exp4 (Figs. 5a and d).
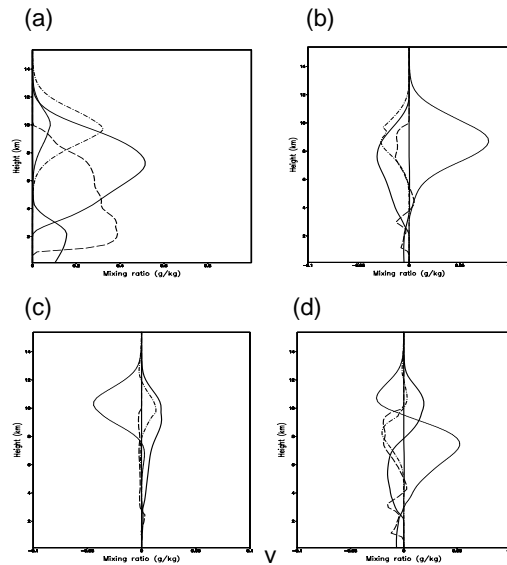
(a)   (b)

(c)   (d)

Fig. 5 Vertical distribution of the domain-averaged water species during the 60min integration period, obtained from the (a) Exp1, (b) Exp2 minus Exp1, (c) Exp3 minus Exp1, and (c) Exp4 minus Exp1 experiments. Units are gkg^{-1} for rain, snow, and graupel, and $10gkg^{-1}$ for cloud ice and cloud water.
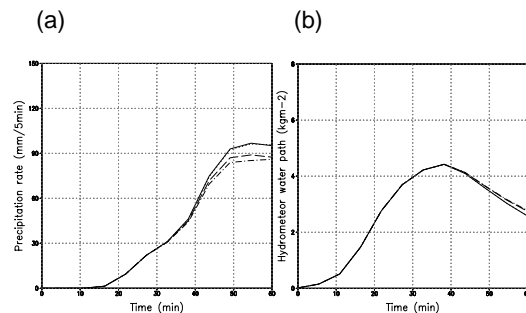
(a)   (b)

Fig. 6 Time series of the precipitation rate (b) hydrometeor water path, resulted from the Exp1 (solid), Exp2 (dashed), Exp3 (dotted), and Exp4 (dot-dashed) experiments over the whole domain.

Less effective melting process of graupel in the Exp2 and Exp4 having less mixing ratio of graupel than the Exp1 experiment at around melting level causes surface precipitation reduced (Fig. 6a).

b. Heavy rainfall event

Figure 7 compares the predicted 24-h accumulated rain valid at 00 UTC 15 July 2001, obtained from the two different experiments (Exp1 and Exp4) at the 5 km resolutions. It is seen that the two experiments capture the observed heavy rainfall extending from southwest to northeast across the central part of the Korean peninsula, with detailed features. The pattern correlation and bias score is not distinctly affected by the changed velocities of hydrometeors, but the maximum precipitation is reduced in the case of Exp4. The new velocities for snow and graupel alleviate excessive precipitation in terms of maximum amount problem that Hong and Lim (2006) pointed out.
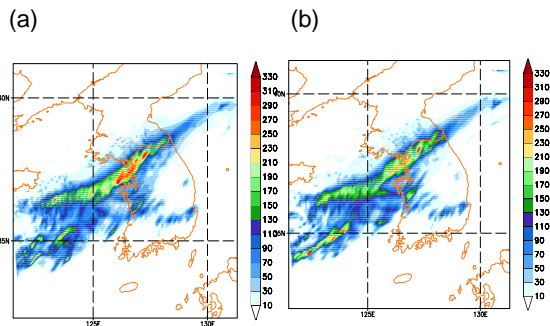
(a)   (b)

Fig. 7 24-hr accumulated rainfall (mm) ending at 0000 UTC 15 July 2001, from the 5-km resolution, obtained from the (a) Exp1 and (b) Exp4 experiment.
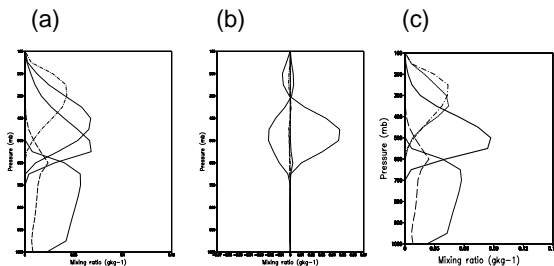
(a)   (b)   (c)

Fig. 8 Vertical distribution of water species, obtained from the (a) Exp1, (b) Exp4, and the (c) difference (Exp4 minus Exp1), averaged over the heavy rainfall region (32.3-41.2 N, 121.5-131.3 E) during the 24-h forecast period.

Figure 8 shows the vertical profiles of averaged condensates over the heavy rainfall region centered in Korea. As in the idealized experiment, snow (graupel) increases (decreases) at around freezing level in the Exp4 experiment. Vertical cross sections of the snow and graupel also show that the new velocities of snow and graupel alleviate the problems of WSM6, that is

reproducing much precipitation in terms of maximum amount when WSM6 scheme is used for heavy rainfall-simulation (not shown).

Figure 9 shows the time-series of precipitation rate and the hydrometeor path computed from the two experiments. Surface precipitation rate is reduced in the Exp4 experiment as forecast time goes by. This result complies with the result obtained in the idealized tests. And In terms of hydrometeor water path, in spite of a more hydrometeor remained, the Exp1 experiment shows small hydrometeor water path because of the greater density of graupel than that of snow.
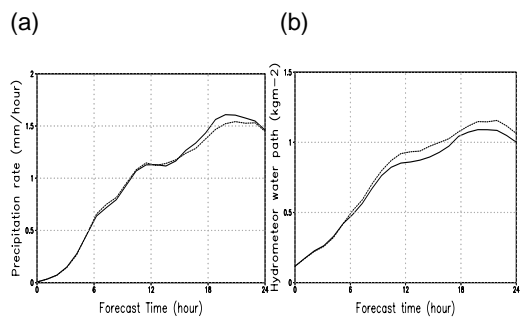
(a)   (b)

Fig. 9 Time series of the (a) surface precipitation rate (mm/5min), and (b) hydrometeor path amount averaged over the domain, resulted from the Exp1 (solid) and Exp4 (dotted) experiments.

4. Summary

This study examined the effect of new mass-weighted sedimentation velocities of snow and graupel in the WSM6 microphysics scheme, based on the observational evidence. Sensitivity tests were carried out for an idealized storm case and a heavy rainfall event over Korea. The new formula increases (decreases) snow (graupel) at the relatively warm temperatures, leading to improving the distribution of hydrometeors as compared with observed data. Also it was found out that the new velocity for graupel and snow alleviates excessive precipitation problem in the WSM6 scheme.

Acknowledgements